

Flux Growth and Characterization of Bulk InVO₄ Crystals

Olesia Voloshyna , Mikhail V. Gorbunov , Daria Mikhailova , Andrey Maljuk, Silvia Seiro and Bernd Büchner

Leibniz IFW Dresden, Helmholtzstr. 20, 01069 Dresden, Germany; m.gorbunov@ifw-dresden.de (M.V.G.); d.mikhailova@ifw-dresden.de (D.M.); a.malyuk@ifw-dresden.de (A.M.); s.seiro@ifw-dresden.de (S.S.); b.buechner@ifw-dresden.de (B.B.)

* Correspondence: o.voloshyna@ifw-dresden.de

Abstract: The flux growth of InVO₄ bulk single crystals has been explored for the first time. The reported eutectic composition at a ratio of V₂O₅:InVO₄ = 1:1 could not be used as a self-flux since no sign of melting was observed up to 1100 °C. Crystals of InVO₄ of typical size 0.5 × 1 × 7 mm³ were obtained using copper pyrovanadate (Cu₂V₂O₇) as a flux, using Pt crucibles. X-ray powder diffraction confirmed the orthorhombic *Cmcm* structure. Rests of the flux material were observed on the sample surface, with occasional traces of Pt indicating some level of reaction with the crucible. X-ray absorption spectroscopy showed that oxidation states of indium and vanadium ions are +3 and +5, respectively. The size and high quality of the obtained InVO₄ crystals makes them excellent candidates for further study of their physical properties.

Keywords: flux growth; indium vanadate; XANES (X-ray absorption near-edge spectroscopy); EXAFS (extended X-ray absorption fine structure)



Citation: Voloshyna, O.; Gorbunov, M.V.; Mikhailova, D.; Maljuk, A.; Seiro, S.; Büchner, B. Flux Growth and Characterization of Bulk InVO₄ Crystals. *Crystals* **2023**, *13*, 1439. <https://doi.org/10.3390/cryst13101439>

Academic Editor: Andrey Prokofiev

Received: 13 September 2023

Revised: 25 September 2023

Accepted: 26 September 2023

Published: 28 September 2023



Copyright: © 2023 by the authors. Licensee MDPI, Basel, Switzerland. This article is an open access article distributed under the terms and conditions of the Creative Commons Attribution (CC BY) license (<https://creativecommons.org/licenses/by/4.0/>).

1. Introduction

Among orthovanadates with the formula M³⁺VO₄ (M³⁺ = In, Fe, Cr, Ti), the InVO₄ compound possesses promising electrochemical and photocatalytic properties for a wide range of commercial applications, e.g., as material for photovoltaic cells for solar energy utilization due to the vanadium 3d band, lying below the analogous d band of other transition metals in the energy spectrum, thus decreasing the band gap; as a photocatalyst, inducing decomposition of water molecules under visible light irradiation; or as an electrode material for lithium-ion batteries.

Several different crystal structures have been reported for InVO₄, depending on the synthesis method, heat treatment conditions, and external pressure. At ambient pressure, the following phases can be obtained: a monoclinic phase InVO₄-I with a α -MnMoO₄-type structure (space group *C12/m1*) [1], an orthorhombic phase InVO₄-III with a CrVO₄-type structure (space group *Cmcm*) [2], and the phase InVO₄-II with undetermined structure [3]. At high pressure, two other phases of InVO₄ have been reported recently: InVO₄-V with a characteristic wolframite-type structure (space group *P12/c*) and InVO₄-IV with an unknown structure, coexisting with phases InVO₄-III and InVO₄-V in the narrow range of pressure between 6.2 GPa and 7.2 GPa [4]. The phase transformation InVO₄-III→InVO₄-V from the orthorhombic CrVO₄-type to the monoclinic wolframite-type structure occurs at a pressure of around 8 GPa and is accompanied by a large volume decrease of 16.6% and a change in coordination number for vanadium atoms from 4 for InVO₄-III to 6 for InVO₄-V [5,6]. These structural transformations trigger a color change of the material and a sudden decrease of the electrical resistivity, related to a band-gap collapse of nearly 1.5 eV [6,7]. Additionally, according to [8], compounds like InVO₄ with six-coordinated vanadium ion may show maximum efficiency for the splitting of water molecules under the visible light. A high-pressure study of the indium vanadate material can provide insights into some physical properties, e.g., dielectric function, refractive index, and absorption

spectra, as well as their practical applications; but so far, such studies have only been performed on polycrystalline samples [4,7]. It is commonly recognized that single crystals provide the best performances compared to polycrystalline samples, and one can expect improved characteristics in single crystals of InVO_4 compared to previously published for polycrystalline samples. The search for the publication, dealing with the single crystal growth of InVO_4 compound, appeared very surprising for authors. Only one paper, where single crystals with dimensions $0.1 \times 0.1 \times 0.3 \text{ mm}^3$ were obtained, was found [2]. Thus, obtaining an InVO_4 bulk single crystal is rather complicated due to the incongruent melting of the indium vanadate [3]. On the other hand, the availability of InVO_4 single crystals should help avoid extrinsic effects due to grain boundaries and reach better hydrostatic conditions for the high-pressure study. Authors were encouraged to find a suitable growth technique for obtaining bulk single crystals of indium vanadate. In the presented work, authors report the successful growth of single crystals of orthorhombic InVO_4 with size $0.5 \times 1 \times 7 \text{ mm}^3$ and the characterization of their ambient pressure properties, preparative to a further high-pressure study.

2. Materials and Methods

2.1. Determination of Flux Composition

The InVO_4 compound melts incongruently at $1134 \text{ }^\circ\text{C}$, according to the phase diagram of the system $\text{In}_2\text{O}_3\text{--V}_2\text{O}_5$ [3]. Thus, single crystals of this material cannot be obtained by direct crystallization from a melt of the stoichiometric composition, where the molar ratio of precursor oxides (In_2O_3 and V_2O_5) is 1:1. In [2], tiny single crystals of InVO_4 ($0.1 \times 0.1 \times 0.3 \text{ mm}^3$) were obtained from a mixture of initial oxides In_2O_3 and V_2O_5 via slow cooling of the mixture from a temperature of $1300 \text{ }^\circ\text{C}$ to the room temperature. An additional challenge is the sublimation of In_2O_3 in air above $1100 \text{ }^\circ\text{C}$ [9,10]. Flux growth is a promising approach but requires finding a suitable flux material; i.e., a material with a melting point lower than that of InVO_4 ($1134 \text{ }^\circ\text{C}$), that does not lead to incorporation of flux ions into the InVO_4 structure, and does not react with or dissolve the crucible material: a melting point of flux well below $1000 \text{ }^\circ\text{C}$ should help avoid the loss of In_2O_3 during growth.

In order to avoid chemical contamination with other ions, the use of a self-flux containing In_2O_3 and V_2O_5 was first explored. Since a low-temperature eutectic with a melting point of $678 \text{ }^\circ\text{C}$ was reported at a ratio of $\text{V}_2\text{O}_5:\text{InVO}_4 = 1:1$ in the $\text{In}_2\text{O}_3\text{--V}_2\text{O}_5$ binary system [3], this composition appeared as a natural flux candidate. However, preliminary experiments for $\text{V}_2\text{O}_5:\text{InVO}_4$ in a 1:1 molar ratio, realized in the optical high-temperature microscope [11], failed to show any melting even up to temperatures around $1100 \text{ }^\circ\text{C}$. Therefore, the phase diagram for the $\text{In}_2\text{O}_3\text{--V}_2\text{O}_5$ binary system in [3] requires revision and additional investigations.

Copper pyrovanadate $\text{Cu}_2\text{V}_2\text{O}_7$ with vanadium ions in a +5 oxidation state was tested next as flux material. This compound melts congruently at around $785 \text{ }^\circ\text{C}$, well below $1000 \text{ }^\circ\text{C}$, and around $350 \text{ }^\circ\text{C}$ lower than the melting point of InVO_4 . Although the close values for the ionic radii of In^{3+} and Cu^{2+} for octahedral oxygen coordination (0.76 \AA and 0.71 \AA , respectively) suggest the possibility of Cu substitution for In in InVO_4 , the different oxidation state of the ions can help prevent it. Besides, according to the ternary phase diagram $\text{CuO--In}_2\text{O}_3\text{--V}_2\text{O}_5$ [12] in the subsolidus region for the compositions with the content of CuO lower than 50 mol.%, only 4 compounds were detected: copper vanadates ($\text{Cu}_2\text{V}_2\text{O}_7$ and CuV_2O_6), indium vanadate (InVO_4), and vanadium oxide (V_2O_5).

2.2. Single Crystal Growth

In_2O_3 (Sigma Aldrich Corp., St. Louis, MO, USA), V_2O_5 , and CuO (Alfa Aesar by Thermo Fisher Scientific GmbH, Hennigsdorf, Germany) with purity not less than 4N were used as starting materials. A mixture was made according to the weight ratio of components $\text{InVO}_4:\text{Cu}_2\text{V}_2\text{O}_7$ (flux) = 1:4. The mixing of oxides was carried out in an agate mortar with ethanol. After mixing, the mixture was dried and placed in a crucible. The flux growth was realized according to the following procedure. The mixture was heated

up to 950 °C with a rate of 150 °C/h with further dwelling at this temperature for 12 h. After homogenization at 950 °C, the melt was slowly cooled down to 800 °C at a rate of 2.5 °C/h, and dwelled at this temperature for 12 h to promote crystallization. After the second dwelling, the molten flux was decanted. The temperature for the homogenization of melt was chosen such that it was above the melting point of the flux (785 °C) and below the point (1100 °C) at which significant intensification of the sublimation of In_2O_3 was detected [9,10].

The first experiment was carried out in an Al_2O_3 -crucible. After finishing the experiment, authors noticed that melt not only reacted with the crucible (Figure 1a), but also attacked the plates placed below it (Figure 1b) in the furnace.

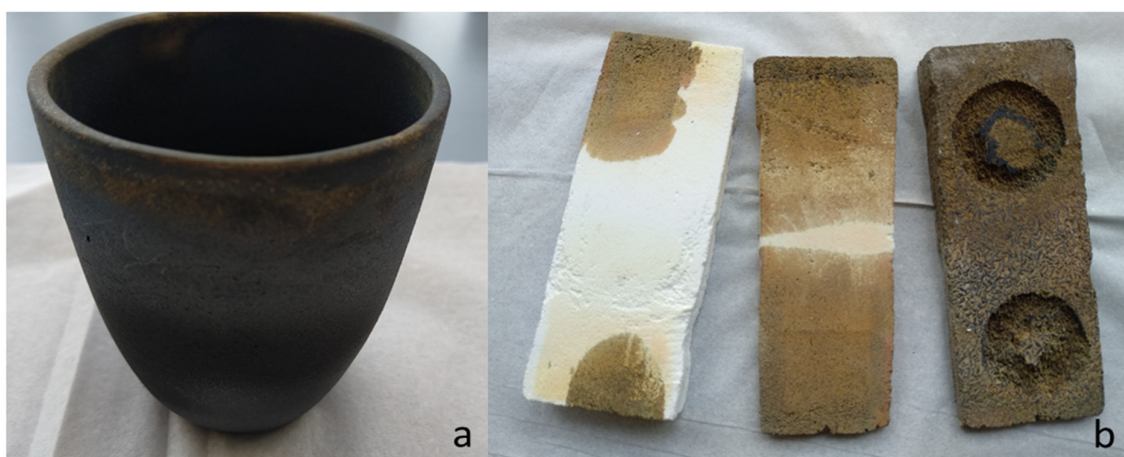


Figure 1. (a) Al_2O_3 -crucible showing chemical reaction with the In_2O_3 - V_2O_5 - CuO melt. The plates under the crucible (b) were also soaked with melt.

Thus, the Al_2O_3 -crucible is not suitable for the flux growth of InVO_4 single crystals with $\text{Cu}_2\text{V}_2\text{O}_7$ as a flux. As well, crucibles made from stabilized zirconia oxide cannot be used for the flux growth due to high probability of being destroyed after rapid cooling. Thus, a Pt-crucible was chosen for carrying out the flux growth of InVO_4 crystals.

As a result, faceted and needle-like crystals have been obtained on the bottom of the crucible after decanting the flux, see Figure 2.

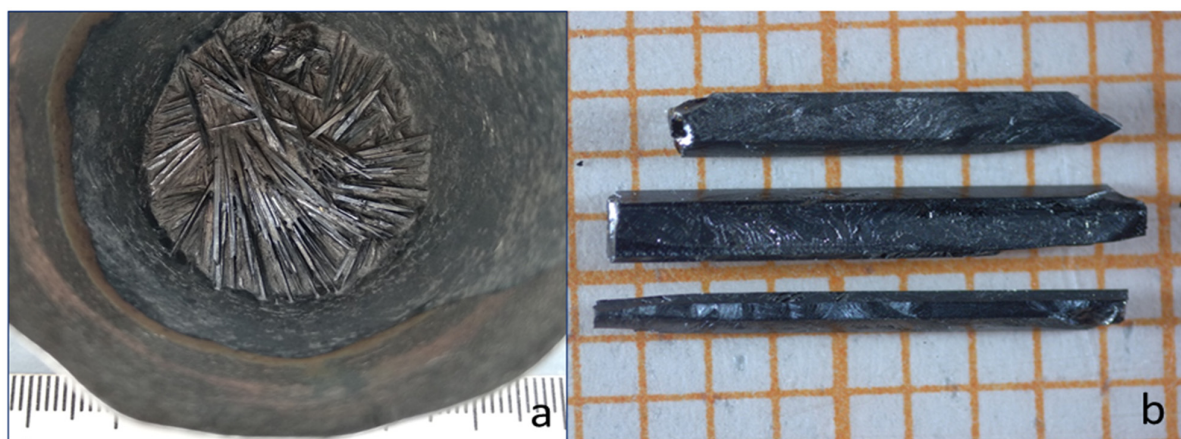


Figure 2. (a) InVO_4 crystals on the bottom of a Pt crucible exposed after decanting the flux. (b) Typical InVO_4 crystals extracted from (a).

For the rare earth orthovanadates, grown by Cz-technique in the inert (Ar) atmosphere, the color of the crystals from yellowish to light brown was linked with the forming of

coloration centers due to a change of the vanadium oxidation state from +5 to +4 and +3 [13,14]. Heat treatment of crystal samples in the air or in the oxygen atmosphere at the 1300 °C for 24 h led to elimination of these coloration centers. Thus, similarly to the rare earth orthovanadates, the heat-treatment of obtained InVO_4 crystals was realized in an oxygen atmosphere at 300 °C for 240 h to eliminate possible color centers in crystals. As it can be seen from Figure 3, the annealing did not lead to a change of the color. Thus, authors assume that black color is the characteristic color of an InVO_4 single crystal.

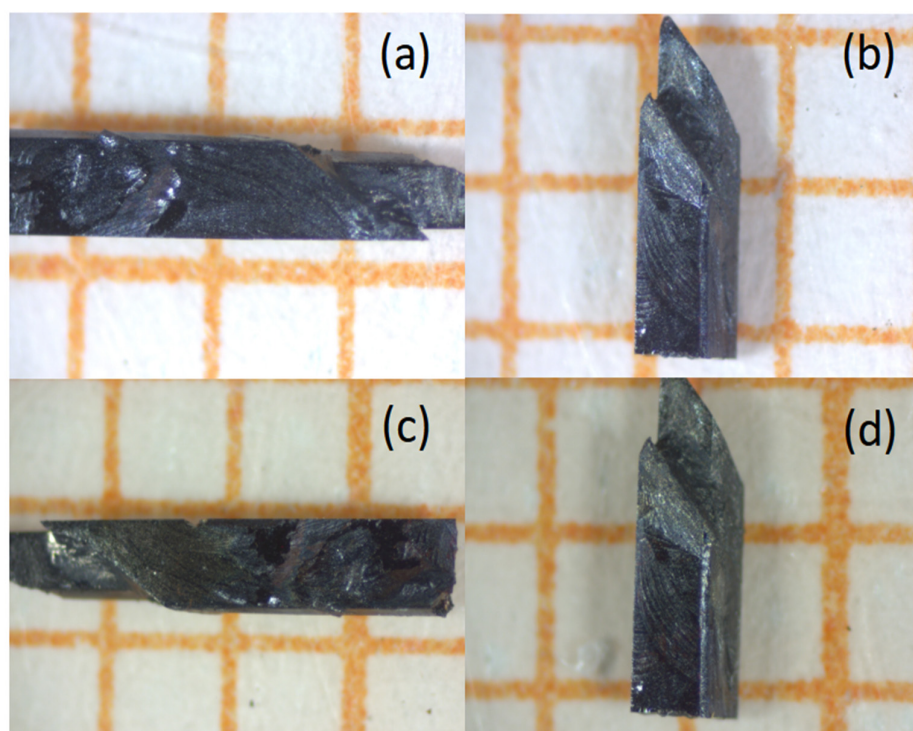


Figure 3. View of InVO_4 crystals before the annealing (a,b) and after annealing (c,d) at 300 °C for 240 h.

2.3. Sample Characterization

X-ray powder diffraction studies on crushed crystals were carried out using an automated powder HUBER diffractometer with $\text{Cu K}\alpha 1$ radiation (Bragg–Brentano geometry, 2θ range from 4° to 100°, step-scanning mode, $\Delta 2\theta = 0.005^\circ$, counting time of 10 s). The Rietveld analysis [15] of the X-ray powder diffraction data was performed with a FullProf program package [16]. For the cell parameter refinement, the atomic positions and cell parameters from [3,17] were used.

Microphotographs of crystals were obtained on a Zeiss Axiocam 105 color microscope camera. Energy-dispersive X-ray analysis (EDX) was performed using an analytical scanning electron microscope Zeiss EVOMA15. The operating voltage was 30 kV. The Cu and V contents were determined using K- and L-lines; for the In-content, L-lines were used. Element analysis of single crystal samples of InVO_4 was realized on iCAP6500 DUO (Thermo Fisher Scientific GmbH, Hennigsdorf, Germany) by method of inductively coupled plasma with optical emission spectrometry (ICP-OES). Before the measurements, samples were dissolved in the mixture of the hydrochloric and hydrofluoric acids with the volume ratio $\text{HCl}:\text{HF} = 8:1$.

X-ray absorption near-edge spectroscopy was applied to determine the oxidation states of indium and vanadium in the InVO_4 single crystals, and to characterize the coordination environment of indium. The experiment was performed using the facilities of P64 beamline of DESY, Hamburg [18]. The monochromator was Si 311 for the In K-edge, and Si 111 for the V K-edge. The In K-edge region was scanned in both transmission and fluorescence

yield modes, whereas the vanadium K-edge region was recorded in fluorescence mode only. Corresponding metallic foils were used for the monochromator energy calibration, and various vanadium oxides served as standards for the corresponding oxidation states. All data processing was conducted in the Demeter software package [19].

Diffuse reflectance spectrum has been measured in the range 200–2000 nm with Shimadzu MPC-3100 UV-vis-NIR spectrophotometer (Shimadzu Deutschland GmbH, Berlin, Germany) using an integrating sphere of a 60 mm diameter. A BaSO₄ compound was used as a reference. The InVO₄ sample was pestled and mixed with BaSO₄ powder.

3. Results and Discussion

3.1. Characterization with X-ray Powder Diffraction and EDX

The analysis of X-ray powder diffraction data (Figure 4) shows that the crystals are composed of orthorhombic InVO₄. Although the presence of a small amount of flux material was observed, no other phases were detected. In particular, no signature of the monoclinic phase of InVO₄ was detected, confirming previously published reports in which the monoclinic phase was found to progressively convert into the orthorhombic by annealing above 600 °C [3,20], and only the orthorhombic phase without traces of additional phases was obtained at temperatures about 800–1000 °C [2].

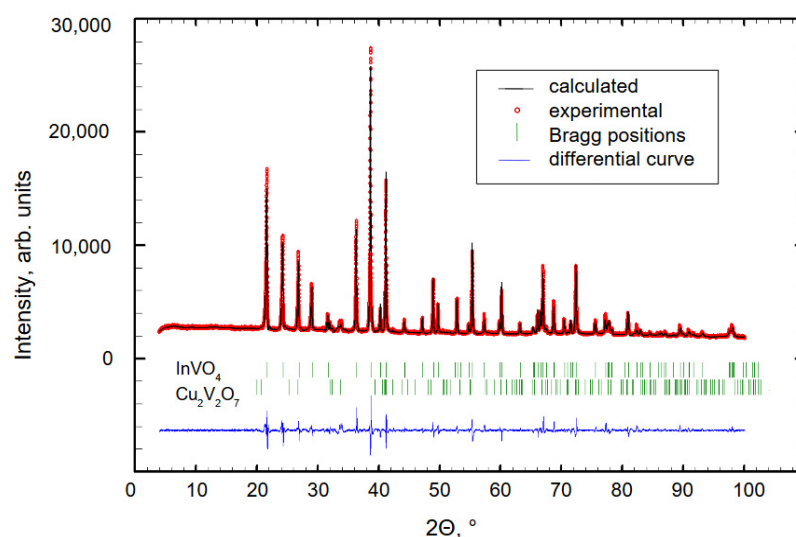


Figure 4. X-ray powder diffraction pattern for crushed InVO₄ crystals. The position of Bragg peaks for InVO₄, for Cu₂V₂O₇ are indicated in green; the difference between calculated (black line) and experimental (red dots) intensities is represented in blue.

Thus, authors obtained crystals of orthorhombic InVO₄ at lower temperatures than was stated in [2]. Such a significant decrease of temperature (350 °C lower than reported in [2]) might lead to obtaining crystals without admixture phases. For instance, in [3], it was stated that for crystals obtained at temperatures higher than 1200 °C, alongside the main phase of InVO₄, admixture phases of V₂O₅ and In₂O₃ have been detected on the X-ray diffraction curves. The cell parameters for InVO₄ determined from our data are presented in Table 1.

Table 1. Refinement data for InVO_4 and $\text{Cu}_2\text{V}_2\text{O}_7$.

| $\text{Cu}_2\text{V}_2\text{O}_7$ | InVO_4 | Parameter |
|--|--|---|
| <i>Fdd2</i> (#43) $\text{Cu}_2\text{V}_2\text{O}_7$ -type | <i>Cmcm</i> (#64) CrVO_4 -type | Space group, Prototype |
| 8.3631(0) | 5.7329(8) | <i>a</i> , Å |
| 20.6495(6) | 8.5010(8) | <i>b</i> , Å |
| 6.4497(6) | 6.5590(3) | <i>c</i> , Å |
| 1113.837(0.000) | 319.664(0.014) | <i>V</i> , Å ³ |
| 114 | 73 | Reflections measured |
| 16.1 | 4.64 | Weighted profile R-factor (<i>R</i> _{wp}) |
| 6.76 | 1.94 | Expected R factor (<i>R</i> _{exp}) |
| 5.69 | 5.69 | Goodness of fit (χ^2) |
| 2.87 | 97.13 | Content in the sample, wt.% |

Scanning electron microscopy images of the crystals in the BSE mode revealed the presence of some areas of different chemical composition, see Figure 5. EDX analysis showed that the darker areas in the images correspond to a small amount of the flux phase ($\text{Cu}_2\text{V}_2\text{O}_7$ with the content of elements according to the EDX analysis: Cu-21.3 at.%; V-22.7 at.%; O-56.0 at.%) on the surface of the crystals, consistent with results from X-ray powder diffraction. The composition of the main phase was consistent with InVO_4 , with the content of elements according to the EDX analysis: In-17.2 at.%; V-16.6 at.%; O-66.2 at.%. Occasionally, tiny bright spots were observed where the presence of Pt was detected (less than 0.1 wt.%) (Figure 5c).

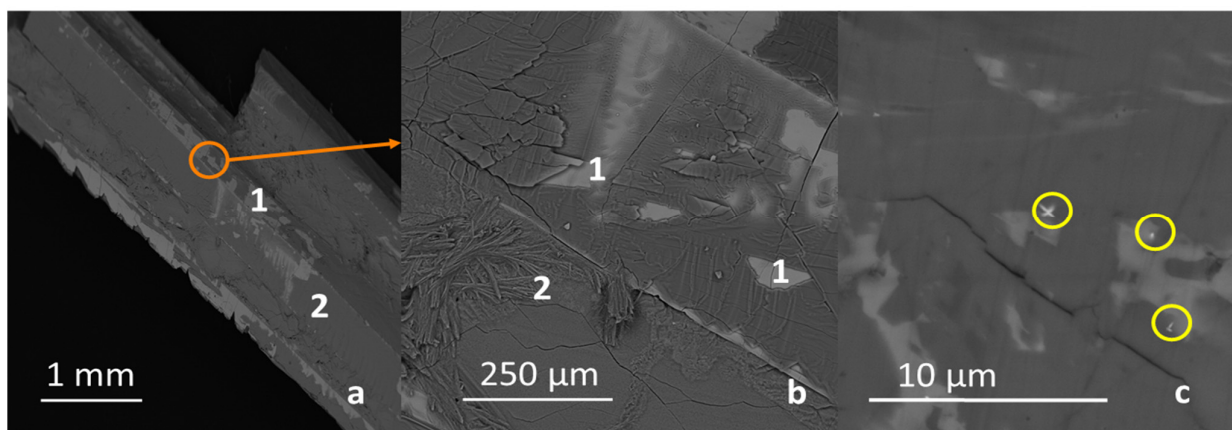


Figure 5. BSEM image of a typical InVO_4 crystal (a) and of crystal surface, marked by orange circle in (a). (b) Here, 1– InVO_4 and 2– $\text{Cu}_2\text{V}_2\text{O}_7$. (c) SEM image of the crystal surface. Tiny inclusions of Pt are highlighted by yellow circles.

According to the ICP-OES results, the content of Pt in the single crystals is lower than 0.01 wt.% and Cu content is 5.13 wt.%. Such high Cu content can be explained by the high relative surface of the needle-like crystals used for the analysis. Noteworthy is that the Cu atom content was determined highly inhomogeneous in the crystal, proving its presence on the surface of the InVO_4 crystals only.

3.2. Characterization with XANES

The X-ray absorption spectra of the InVO_4 single crystal at the In and V K-edge regions are shown in Figure 6.

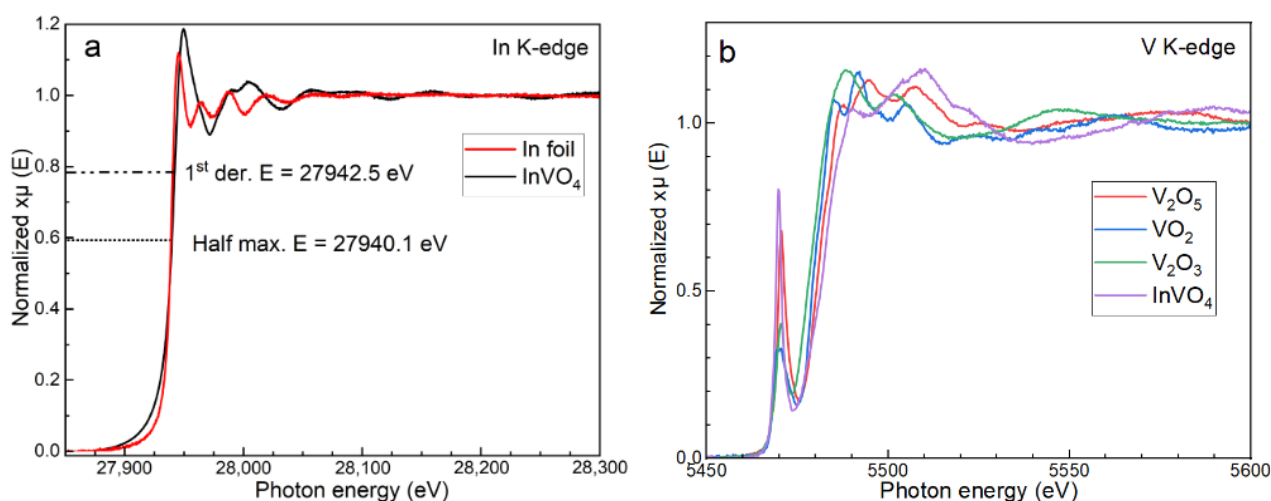


Figure 6. Normalized absorption of InVO₄ single crystal in (a) In and (b) V K-edge regions.

The In K-edge energy position was defined by applying the first derivative method [21]. No pre-edge features are observed, as In³⁺ has a completely occupied 4d-shell, and the main edge corresponds to the 1s→5p electronic transition. The edge energy E_0 of 27,939.9 eV for the In-foil was used for calibration [22]. The In K-edge energy position for InVO₄ at 27,942.5 eV is 2.6 eV higher than for metallic indium, since the effective core charge increases in In³⁺ compared to In⁰ with simultaneous rise of the binding energy of the core electrons (see Figure 7).

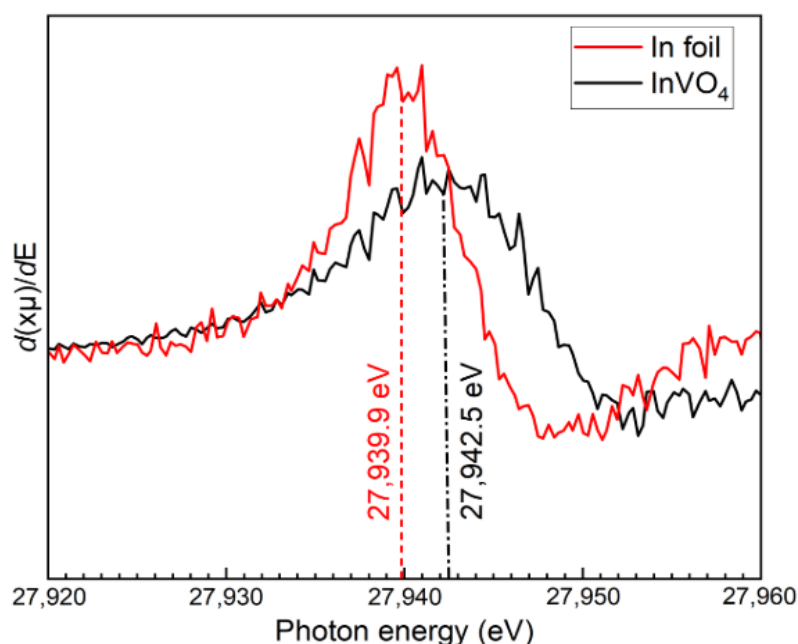


Figure 7. First derivative of In K-edge region of X-ray absorption spectra for InVO₄ and In foil.

Note that various possibilities of estimating the element K-edge position are known in the literature; for example, the value at half of the normalized $x\mu(E)$ step. For InVO₄, it corresponds to about 27,940.1 eV, as demonstrated in Figure 6a, which agrees with the energy position reported in [23] for In₂O₃. This confirms a +3 oxidation state in our InVO₄ single crystals.

In the case of vanadium, the pre-edge feature, which corresponds to the 1s→3d electron transition, is observed. Its shape is known to be sharp, and its intensity is comparable with the intensity of the main edge 1s→4p transition for V⁵⁺ containing compounds [24].

Thus, the observed pre-edge feature for InVO_4 can be considered as a confirmation for the V^{5+} presence in InVO_4 single crystals, similarly to that observed previously in BiVO_4 [25]. It is considered that the position of the main edge depends linearly on the oxidation state of the ion, assuming a similar coordination number. Vanadium oxides perfectly follow this trend; however, the vanadium K-edge lays at a higher energy for InVO_4 compared to that for V_2O_5 . The possible explanation for such an effect is the different coordination for vanadium ions: octahedral in V_2O_5 , while in InVO_4 the coordination is tetrahedral. Therefore, summarizing obtained XANES results, authors can unequivocally conclude that vanadium is present in the oxidation state as V (+5) in InVO_4 single crystals.

3.3. EXAFS (Extended X-ray Absorption Fine Structure)

Based on the structural model of InVO_4 and high-quality XAS data obtained for the indium K-edge, we have determined the local structural surrounding for In-cations, based on photoelectron scattering on the nodes of the crystal lattice. For this, the absorption data were normalized, converted into a reciprocal k-space (k is a wavenumber per length unit, zero is set at the defined position of the absorption edge), followed by the Fourier-transformation into R-space as a k^3 -weighted data. Multiplying the EXAFS function $\chi(k)$ by k^n allows to amplify the oscillations, especially at higher k, since their intensity decays very fast with its increase [26]. The theoretical EXAFS function was calculated using the structural model of the InVO_4 , and least square fitting is performed, allowing estimation of the interatomic distances within the first few coordination spheres of the absorbing atom. The procedure of fitting is automated and known as FEFF code [27] and implied in Demeter software [19]. The results of these calculations are shown in Figure 8.

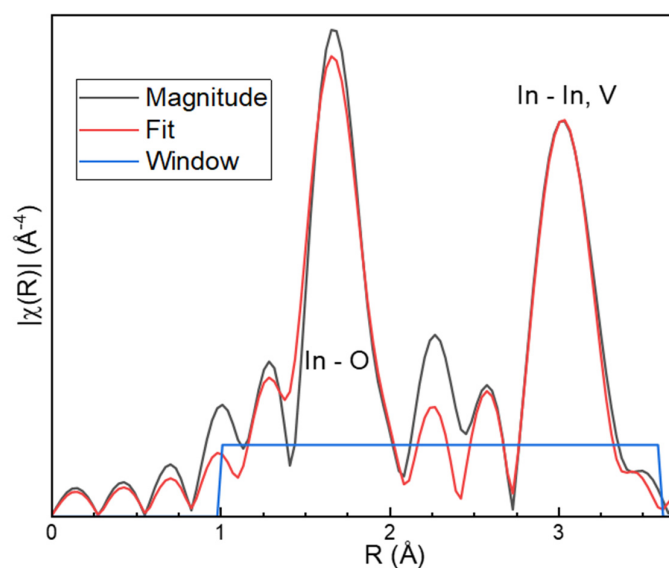


Figure 8. Part of the Fourier-transformed In K-edge EXAFS function of InVO_4 single crystal together with the same function based on the crystallographic model.

The intense local maxima in the oscillations reflect the scattering of photoelectrons on the atoms belonging to the closest coordination spheres of indium. Since indium-oxygen tetrahedrons are distorted, two bonds of different lengths provide the first big, slightly asymmetric peak. The second peak is formed by the In–In scattering path, while the small shoulder at 3.4 Å can be attributed to the In–V distance. It is difficult to distinguish visually between the In–O3 and In–V oscillations; however, adding them both to the calculation model allows to realize a proper fit. Table 2 shows the results of the calculations.

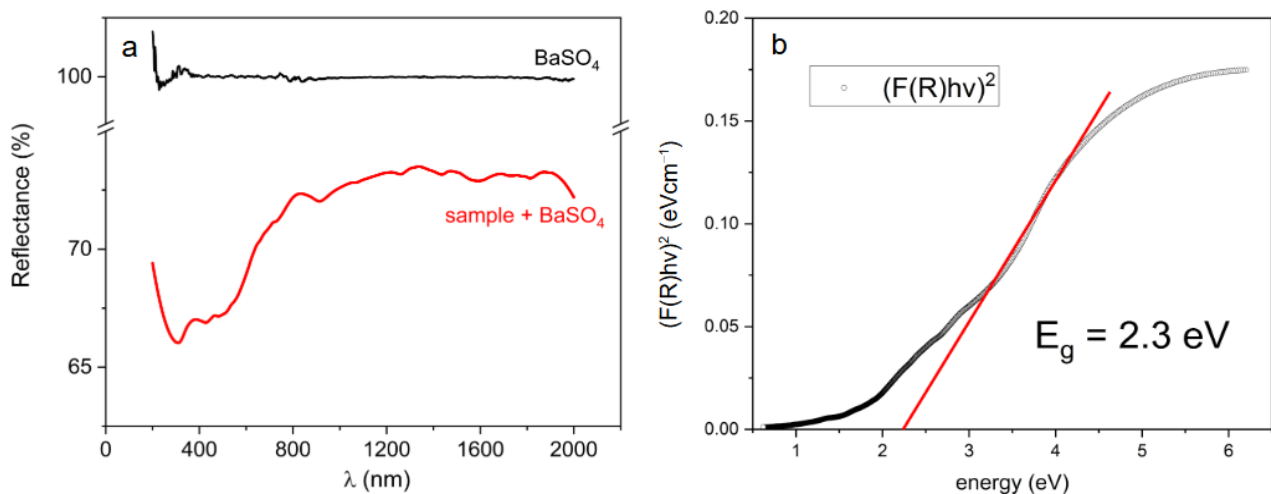
Table 2. Comparison of data for InVO₄ single crystal obtained based on Rietveld refinement and EXAFS calculations.

| | EXAFS Calc. | Str. Model | Distance (in Å) |
|---------------|-------------|------------|-----------------|
| $R_f = 0.036$ | 2.11(4) | 2.1184 | In–O1(×4) |
| | 2.22(6) | 2.2219 | In–O2(×2) |
| | 3.29(2) | 3.2795 | In–In |
| | 3.53(9) | 3.4985 | In–V |

As one may see, the values obtained from the EXAFS fitting match well to the values from the structural model, proving a high quality of obtained InVO₄ single crystals. The quality of obtained InVO₄ crystals is sufficient for further X-ray diffraction study under high pressure, which are realized at pressure values up to 20 GPa with the application of diamonds with a 600 μm culet and at a temperature from RT to 15 K.

3.4. UV-vis-NIR spectroscopy Absorption

In Figure 9a, a diffuse reflectance spectrum of the InVO₄ single crystal is shown.

**Figure 9.** Diffuse reflectance spectrum of the InVO₄ single crystal (a) and Kubelka–Munk transformation for the direct band gap $[(F(R) \times hv)^2]$ (b).

As it can be seen from the spectrum, the InVO₄ single crystal possesses an intense absorption in the region from 200 to 600 nm, confirming previously published results for polycrystalline samples [28,29]. The InVO₄ single crystal shows an absorption in the visible light region, supporting the promising photocatalytic activity, determined previously for the polycrystalline samples in [28,29].

Results for the transformation of the reflectance spectroscopic data by the Kubelka–Munk model are presented in Figure 9b. The transformation has been realized for the direct band gap $[(F(R) \times hv)^2]$, where $F(R)$ is the Kubelka–Munk equation, cm^{-1} and hv is an energy, eV. Linear extrapolation of the data in the range from 3 eV to 4.5 eV gives the value of the direct band gap 2.3 eV. There is another linear area in the range from 2 eV to 3 eV on the Kubelka–Munk transformation curve (Figure 9b). Since this absorption is rather weak, it can be caused by the absorption of defect levels below the conduction band. It is noteworthy that for the indirect band-gap transformation $[(F(R) \times hv)^{1/2}]$, no linear areas have been observed on the curve.

It is also noteworthy that for the InVO₄ polycrystalline samples, obtained by solid-state synthesis, the band gap was detected at approx. 2 eV [28], and for the thin-films, at around 3 eV [30,31]. The value of approx. 3 eV was determined by theoretical calculations

for InVO₄ [5,32]. These deviations in the values of determined band gaps might be caused by the different methods of the band-gap determination. For instance, in [31], the band gap for InVO₄ has been determined by the Kubelka–Munk transformation of the optical absorption data for the indirect band gap (3.2 eV), contrary to our data of the direct band gap (2.3 eV). According to [6,7], the drop of the band gap in InVO₄ under the high pressure is around 1.5 eV. Thus, this phenomenon can lead to a pressure-driven metallization at pressures beyond those of the structure transformation.

4. Conclusions

Single crystals of InVO₄ of several mm in length have been grown by a flux-method technique using copper pyrovanadate as a flux (Cu₂V₂O₇). The crystals present the orthorhombic *Cmcm* phase and are pure, except for rests of the flux observed in both X-ray powder diffraction (<3 wt.%), EDX, and ICP-OES. The oxidation states of the indium and vanadium ions are found to be +3 and +5, respectively. EXAFS data are consistent with the used structural model. The determined direct band gap of InVO₄ single crystals is 2.3 eV.

The quality of obtained InVO₄ crystals is sufficient for further studies under high pressure, which are already in progress by the group led by Prof. Dr. J. Geck in TU Dresden, Germany.

Author Contributions: Methodology, O.V. and A.M.; software, M.V.G. and D.M.; formal analysis, M.V.G. and D.M.; investigation, O.V.; resources, O.V. and A.M.; data curation, O.V. and D.M.; writing—original draft preparation, O.V. and M.V.G.; writing—review and editing, A.M., D.M. and S.S.; supervision, A.M. and D.M.; project administration, S.S. and B.B.; funding acquisition, S.S. and B.B. All authors have read and agreed to the published version of the manuscript.

Funding: This research was partly supported by the UKRATOP project funded by the Federal Ministry of Education and Research (BMBF) under reference 01DK18002 and by the Philipp Schwartz Initiative of the Alexander von Humboldt Foundation.

Data Availability Statement: The data presented in this study are available on request from the corresponding author.

Acknowledgments: Authors appreciate the help of V.V.Romaka (IFW, Dresden) with Rietveld refinement for obtained X-ray powder diffraction measurements, of Robert Kluge (IFW, Dresden) with EDX measurements, and of Andrea Voß (IFW, Dresden) with ICP-OES measurements. Authors would like to thank Sandra Schiemenz and Evgenia Dmitrieva (IFW, Dresden) for the UV-vis-NIR measurements. The publication of this article was funded by the Open Access Fund of the Leibniz Association.

Conflicts of Interest: The authors declare no conflict of interest.

References

1. Touboul, M.; Melghit, K.; Bénard, P.; Louër, D. Crystal Structure of a Metastable Form of Indium Orthovanadate, InVO₄-I. *J. Solid State Chem.* **1995**, *118*, 93–98. [[CrossRef](#)]
2. Touboul, M.; Tolédano, P. Structure du vanadate d'indium: InVO₄. *Acta Cryst. B* **1980**, *36*, 240–245. [[CrossRef](#)]
3. Touboul, M.; Ingrain, D. Synthèses et propriétés thermiques de InVO₄ et TlVO₄. *J. Less Common Met.* **1980**, *71*, 55–62. [[CrossRef](#)]
4. Errandonea, D.; Gomis, O.; Garcia-Domene, B.; Pellicer-Porres, J.; Katari, V.; Achary, S.N.; Tyagi, A.K.; Popescu, C. New polymorph of InVO₄: A high-pressure structure with six-coordinated vanadium. *Inorg. Chem.* **2013**, *52*, 12790–12798. [[CrossRef](#)] [[PubMed](#)]
5. Mondal, S.; Appalakondaiah, S.; Vaitheeswaran, G. High pressure structural, electronic, and optical properties of polymorphic InVO₄ phases. *J. Appl. Phys.* **2016**, *119*, 085702. [[CrossRef](#)]
6. Errandonea, D. High pressure crystal structures of orthovanadates and their properties. *J. Appl. Phys.* **2020**, *128*, 040903. [[CrossRef](#)]
7. Botella, P.; Errandonea, D.; Garg, A.B.; Rodriguez-Hernandez, P.; Muñoz, A.; Achary, S.N.; Vomiero, A. High-pressure characterization of the optical and electronic properties of InVO₄, InNbO₄, and InTaO₄. *SN Appl. Sci.* **2019**, *1*, 389. [[CrossRef](#)]
8. Zou, Z.; Ye, J.; Sayama, K.; Arakawa, H. Direct splitting of water under visible light irradiation with an oxide semiconductor photocatalyst. *Nature* **2001**, *414*, 625. [[CrossRef](#)]
9. Liu, Y.; Ren, W.; Shi, P.; Liu, D.; Liu, M.; Jing, W.; Tian, B.; Ye, Z.; Jiang, Z. Preparation and thermal volatility characteristics of In₂O₃/ITO thin film thermocouple by RF magnetron sputtering. *AIP Adv.* **2017**, *7*, 115025. [[CrossRef](#)]
10. Lamoreaux, R.H.; Hildenbrand, D.L.; Brewer, L. High-Temperature Vaporization Behavior of Oxides II. Oxides of Be, Mg, Ca, Sr, Ba, B, Al, Ga, In, Tl, Si, Ge, Sn, Pb, Zn, Cd and Hg. *J. Phys. Chem. Ref. Data* **1987**, *16*, 419–443. [[CrossRef](#)]

11. Nakamura, S.; Maljuk, A.; Maruyama, Y.; Nagao, M.; Watauchi, S.; Hayashi, T.; Anzai, Y.; Furukawa, Y.; Ling, C.D.; Deng, G.; et al. Growth of LiCoO₂ single crystals by the TSFZ method. *Cryst. Growth Des.* **2019**, *19*, 415–420. [[CrossRef](#)]
12. Bosacka, M.; Filipek, E.; Paczesna, A. Unknown phase equilibria in the ternary oxide V₂O₅-CuO-In₂O₃ system in subsolidus area. *J. Therm. Anal. Calorim.* **2016**, *125*, 1161–1170. [[CrossRef](#)]
13. Nobe, Y.; Takashima, H.; Katsumata, T. Decoloration of yttrium orthovanadate laser host crystals by annealing. *Opt. Lett.* **1994**, *19*, 1216–1218. [[CrossRef](#)] [[PubMed](#)]
14. Voloshyna, O.V.; Baumer, V.N.; Bondar, V.G.; Kurtsev, D.A.; Gorbacheva, T.E.; Zenya, I.M.; Zhukov, A.V.; Sidletskiy, O.T. Growth and scintillation properties of gadolinium and yttrium orthovanadate crystals. *Nucl. Instrum. Methods Phys. Res. A* **2012**, *664*, 299–303. [[CrossRef](#)]
15. Rietveld, H.M. A profile refinement method for nuclear and magnetic structures. *J. Appl. Cryst.* **1969**, *2*, 65–71. [[CrossRef](#)]
16. Rodriguez-Carvajal, J.; Roisnel, T. FullProf.98 and WinPLOTR: New Windows95/NT Applications for Diffraction. *IUCr Com. Powder Diffr. Newsl.* **1998**, *20*, 35–36.
17. Calvo, C.; Faggiani, R. α -Cupric vanadate. *Acta Crystallogr. Sect. B* **1975**, *31*, 603–605. [[CrossRef](#)]
18. Caliebe, W.A.; Murzin, V.; Kalinko, A.; Görlitz, M. High-flux XAFS-beamline P64 at PETRA III. *AIP Conf. Proc.* **2019**, *2054*, 060031. [[CrossRef](#)]
19. Ravel, B.; Newville, M. ATHENA, ARTEMIS, HEPHAESTUS: Data analysis for X-ray absorption spectroscopy using IFEFFIT. *J. Synchr. Rad.* **2005**, *12*, 537–541. [[CrossRef](#)]
20. Denis, S.; Baudrin, E.; Touboul, M.; Tarascon, J.-M. Synthesis and electrochemical properties vs Li of amorphous vanadates of general formula RVO₄ (R = In, Cr, Al, Fe, Y). *J. Electrochem. Soc.* **1997**, *144*, 4099–4109. [[CrossRef](#)]
21. Vitova, T.; Mangold, S.; Paulmann, C.; Gospodinov, M.; Marinova, V.; Mihailova, B. X-ray absorption spectroscopy of Ru-doped relaxor ferroelectrics with a perovskite-type structure. *Phys. Rev. B Condens. Matter Mater. Phys.* **2014**, *89*, 144112. [[CrossRef](#)]
22. Bearden, J.A.; Burr, A.F. Reevaluation of X-ray Atomic Energy Levels. *Rev. Mod. Phys.* **1967**, *39*, 125. [[CrossRef](#)]
23. Tsoukalou, A.; Abdala, P.M.; Armutlulu, A.; Willinger, E.; Fedorov, A.; Müller, C.R. Operando X-ray Absorption Spectroscopy Identifies a Monoclinic ZrO₂:In Solid Solution as the Active Phase for the Hydrogenation of CO₂ to Methanol. *ACS Catal.* **2020**, *10*, 10060–10067. [[CrossRef](#)]
24. Chaurand, P.; Rose, J.; Briois, V.; Salome, M.; Proux, O.; Nassif, V.; Olivi, L.; Susini, J.; Hazemann, J.-L.; Bottero, J.-Y. New Methodological Approach for the Vanadium K-Edge X-ray Absorption Near-Edge Structure Interpretation: Application to the Speciation of Vanadium in Oxide Phases from Steel Slag. *J. Phys. Chem. B* **2007**, *111*, 5101–5110. [[CrossRef](#)]
25. Nga, T.T.T.; Huang, Y.-C.; Chen, J.-L.; Chen, C.-L.; Lin, B.-H.; Yeh, P.-H.; Du, C.-H.; Chiou, J.-W.; Pong, W.-F.; Arul, K.T.; et al. Effect of Ag-Decorated BiVO₄ on Photoelectrochemical Water Splitting: An X-ray Absorption Spectroscopic Investigation. *Nanomaterials* **2022**, *12*, 3659. [[CrossRef](#)] [[PubMed](#)]
26. Newville, M. *Fundamentals of XAFS*; Revision 1.7; University of Chicago: Chicago, IL, USA, 2004.
27. Rehr, J.J.; de Leon, J.M.; Zabinsky, S.I.; Albers, R.C. Theoretical X-ray Absorption Fine Structure Standards. *J. Am. Chem. Soc.* **1991**, *113*, 5135–5140. [[CrossRef](#)]
28. Ye, J.; Zou, Z.; Arakawa, H.; Oshikiri, M.; Shimoda, M.; Matsushita, A.; Shishido, T. Correlation of crystal and electronic structures with photophysical properties of water splitting photocatalysts InMO₄ (M=V⁵⁺, Nb⁵⁺, Ta⁵⁺). *J. Photochem. Photobiol. A* **2002**, *148*, 79–83. [[CrossRef](#)]
29. Ye, J.; Zou, Z.; Oshikiri, M.; Matsushita, A.; Shimoda, M.; Imai, M.; Shishido, T. A novel hydrogen-evolving photocatalyst InVO₄ active under visible light irradiation. *Chem. Phys. Lett.* **2002**, *356*, 221–226. [[CrossRef](#)]
30. Oshikiri, M.; Boero, M.; Ye, J.; Zou, Z.; Kido, G. Electronic structures of promising photocatalysts InMO₄ (M=V, Nb, Ta) and BiVO₄ for water decomposition in the visible wavelength region. *J. Chem. Phys.* **2002**, *117*, 7313. [[CrossRef](#)]
31. Enache, C.S.; Lloyd, D.; Damen, M.R.; Schoonman, J.; van de Krol, R. Photo-electrochemical Properties of Thin-Film InVO₄ Photoanodes: The Role of Deep Donor States. *J. Phys. Chem. C* **2009**, *113*, 19351–19360. [[CrossRef](#)]
32. Oshikiri, M.; Boero, M.; Ye, J.; Aryasetiwan, F.; Kido, G. The electronic structure of the thin films of InVO₄ and TiO₂ by first principles calculations. *Thin Solid Films* **2003**, *445*, 168–174. [[CrossRef](#)]

Disclaimer/Publisher's Note: The statements, opinions and data contained in all publications are solely those of the individual author(s) and contributor(s) and not of MDPI and/or the editor(s). MDPI and/or the editor(s) disclaim responsibility for any injury to people or property resulting from any ideas, methods, instructions or products referred to in the content.